ChemComm

Valence-Driven Colorimetric Detection of Norovirus Protease via Peptide-AuNP Interaction

Journal:	*ChemComm*
Manuscript ID	CC-COM-08-2023-004142.R1
Article Type:	Communication

ARTICLE

Valence-Driven Colorimetric Detection of Norovirus Protease via Peptide-AuNP Interaction

Received 00th January 20xx,
Accepted 00th January 20xx

DOI: 10.1039/x0xx00000x

Chuxuan Ling,[a] Zhicheng Jin,[a] Justin Yeung,[b] Elany Barbosa da Silva,[c] Yu-Ci Chang,[d] Tengyu He,[d] Wonjun Yim,[d] Anthony J. O'Donoghue,[c] Jesse V. Jokerst[a,d,e*]

We report here a colorimetric method for rapid detection of norovirus based on the valence-driven peptide-AuNP interactions. We engineered a peptide sequence named K1 with a cleavage sequence in between two lysine residues. The positively charged lysine groups aggregated the negatively charged nanoparticles leading to a purple color change. There was a red color when the cleavage sequence was digested by the Southampton norovirus 3C-like protease (SV3CP)—a protease involved in the life cycle of Human norovirus (HNV). The limit of detection was determined to be 320 nM in Tris buffer. We further show that the sensor has good performance in exhaled breath condensate, urine, and faecal matter. This research provides a potential easy and quick way to selectively detect HNV.

Introduction

Human norovirus (HNV) is a primary cause of foodborne illnesses with more than 600 million cases annually.[1] In contrast to other bacterial foodborne illnesses spread through contaminated food, norovirus is highly contagious[2] and can be transmitted between people.[3] Thus, there is an urgent need for a rapid and accurate detection method for noroviruses. However, current PCR-based detection suffers from bulky equipment and long turnaround times.[4]

Colorimetric detection with gold nanoparticles (AuNPs) has value in many diagnostic applications via the localized surface plasmon resonance;[5-7] this approach can offer high analytical sensitivity with limited specialized equipment.[5] AuNPs-based colorimetric approaches often require a target-activatable reagent to induce the colour change and have included adenosine triphosphate, dopamine, glucose, and amino acids.[8] Oligopeptides are particularly appealing for viral detection due to their specific response to viral proteases.

Here, we report a method for colorimetric detection of the Southampton norovirus 3C-like protease (*i.e.*, SV3CP) via a valence-driven peptide-AuNP interaction. SV3CP is specific to norovirus and is a crucial enzyme in the norovirus lifecycle.[3,9] Sensing uses oligopeptides can be rationally designed to be cleavable by SV3CP. This cleavage changes the oligopeptides' properties (*e.g.*, charge valence), which in turn govern the stability of AuNP colloids. This in turn leads to a colour change that is directly indicative of the presence of SV3CP.[10,11]

We hypothesized that changes in the charge valence on the peptide would alter AuNPs aggregation. We validated our hypothesis by comparing the sensing peptide to several control peptides and then monitoring the interparticle interactions. The particles are red in the presence of protease (no aggregation) and are blue/purple in the absence of protease (aggregation). Control peptides without charge valence change after proteolysis confirm the role of charge valence in colour change. The detection limit was 320 nM for SV3CP in Tris buffer. We further validated the sensor's performance in biological matrices such as urine and faecal matter. This selective, easy-to-use, and label-free biosensor can provide a potential solution for rapid norovirus testing and offers valuable guidance for mitigating its person-to-person transmission.

Results and discussion

We used diphenylphosphinobenzene sulfonate (DPPS)-modified AuNPs and positively charged peptides. The negative sulfonated DPPS ligands make the AuNPs colloidally stable via electrostatic double-layer repulsions.[12,13] However, the surface potential is neutralized when positively charged peptides are introduced into the NP dispersion and reach the critical coagulation concentration (CCC)—this is the concentration at which there is a 50% change in aggregation; this leads to particle aggregation and a colour change when no protease is present.[11] The Schulze-Hardy rule states that the CCC is significantly influenced by the charge valency (z) of counterions, *i.e.*, $CCC \propto$

[a] *Department of Nano and Chemical Engineering, University of California, San Diego, La Jolla, CA 92093, United States*
[b] *Department of Bioengineering, University of California, San Diego, La Jolla, CA 92093, United States*
[c] *Skaggs School of Pharmacy and Pharmaceutical Sciences, University of California, San Diego, La Jolla, CA 92093, United States*
[d] *Program in Materials Science and Engineering, University of California, San Diego, La Jolla, CA 92093, United States*
[e] *Department of Radiology, University of California, San Diego, La Jolla, CA 92093, United States*
*Corresponding author's email: jjokerst@ucsd.edu
Electronic Supplementary Information (ESI) available: [details of any supplementary information available should be included here]. See DOI: 10.1039/x0xx00000x

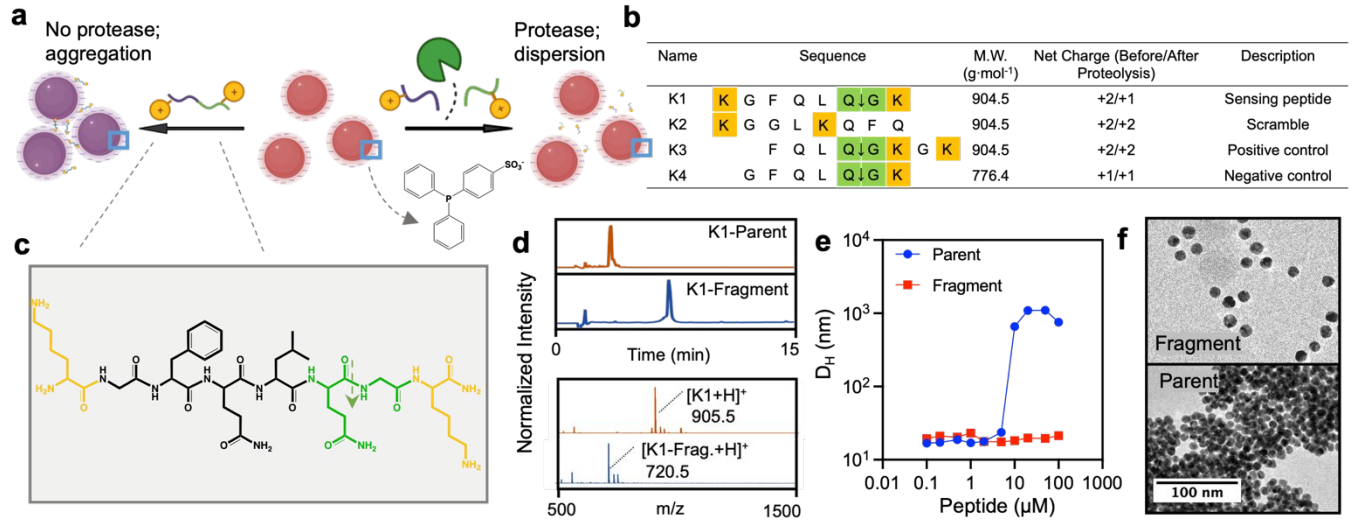

Figure 1. Colour change behaviour of AuNPs with programmed peptides. (a) Schematic illustration of the plasmonic sensing with DPPS-AuNPs; the green cartoon represents SV3CP; yellow circles represent the positively charged domain, flanking the cleavage site. **(b)** Peptide design and information. **(c)** Chemical structure of peptide K1. The green represents the cleavage site, and the yellow represents the positive domain. **(d)** HPLC (top) and MALDI-MS (bottom) data confirm the cleavage of K1 peptide by SV3CP. **(e)** DLS profiles of DPPS-AuNPs incubating with increasing concentration of K1 parent peptide (blue) and fragment peptide (red). **(f)** TEM images of the monodispersed AuNPs in the presence of K1 fragment (top) and aggregated AuNPs in the presence of parent K1 (bottom).

Z[6].[11] Thus, we designed a peptide (named K1) with two positively charged lysine residues (K) located at both the N- and C- terminals and flanking the SV3CP cleavage sequence. The proteolysis of K1 results in fragments carrying only one positive charge valence (**Fig. 1a-c**). Thus, the AuNPs produce a red colour in the presence of SV3CP and a blue/purple colour without SV3CP (**Fig. 1a**).

The successful synthesis and proteolysis of K1 were confirmed with high-performance liquid chromatography (HPLC) and matrix-assisted laser desorption ionization mass spectrometry (MALDI-MS) (**Fig. 1d**). We examined the size change of AuNPs during aggregation induced by the K1 peptide. Dynamic light scattering (DLS) profiles show that AuNPs with a hydrodynamic size of 17 nm rapidly grow to about 1,000 nm in the presence of K1; the CCC is 10 μM (**Fig. 1e**). Conversely, no coagulation is observed when the fragment K1 was introduced below 100 μM. Transmission electron microscopy (TEM) images further confirm the aggregation and dispersion with K1 parent and fragment, respectively (**Fig. 1f**).

We further characterized the interaction between peptides and AuNPs by optical spectroscopy. The ultraviolet-visible (UV-Vis) absorbance spectrum shows a red shift of the peak from 520 nm to 600 nm (**Fig. 2a**). We defined the ratiometric signal Abs_{600}/Abs_{520} as an indicator of aggregation and used it to quantify the colour change. The time-dependent ratiometric signal quantitively shows the aggregation kinetics and colour changes (**Fig. 2b**). The aggregation kinetics strongly correlate with the peptide concentration, and the curves plateau within 60 min. Subsequent analysis measured the colour change at 30 min for consistency, simplicity, and speed. Visual inspection and photographs of the AuNP solutions confirm the spectroscopy data (**Fig. 2c**): The colour changes from red to purple. The colour change becomes more pronounced with increasing peptide concentration and incubation time. AuNPs incubated with fragment K1 remain red because there is no charge-based cross-linking/aggregation, thus indicating the presence of the protease biomarker.

To optimize the sensor performance and examine the aggregation mechanism, we first examined AuNPs with a series of phosphine sulfonate ligands (**Fig. S3**): DPPS, bis(p-sulfonatophenyl)phenylphosphine (BSPP), and triphenylphosphine-3,3,3-trisulfonic acid (TPPTS). These ligands have an increasing number of sulfonate groups from 1 to 3, resulting in more negative surface potential: $\zeta_{(DPPS\text{-}AuNPs)} < \zeta_{(BSPP\text{-}AuNPs)} < \zeta_{(TPPTS\text{-}AuNPs)}$ (**Table 1**). In principle, the most negatively charged TPPTS-AuNPs would have a larger working window due to the high colloidal stability enhanced by the strong electrostatic double layer repulsion.[11] However, the DPPS-AuNPs actually exhibited a wider working window and were selected for subsequent investigations (**Fig. S4a**). We attributed this unexpected result to the strong affinity of this specific peptide sequence to TPPTS-AuNPs.

Fig. 1b details the sequences of the sensing peptides and other control peptides that further verified the mechanism of charge valence as the key determinant of aggregation. One reported cleavage sequence for SV3CP is EFQLQ↓GK.[14] This work excluded the Glu (E) at P_5' because its negative charge may interrupt the overall electrophoretic property of the peptide. We confirmed that this Glu is not a critical amino acid for a cleavage by SV3CP (**Fig. 1d**). The positively charged Lys (K) is in the cleavage sequence and is crucial for proteolytic cleavage.[14]

Table 1. Zeta potential of AuNPs coated with different ligands.

Ligand	Zeta potential (mV)
DPPS	-19.6 ± 1.0
BSPP	-22.7 ± 0.9
TPPTS	-39.8 ± 7.0

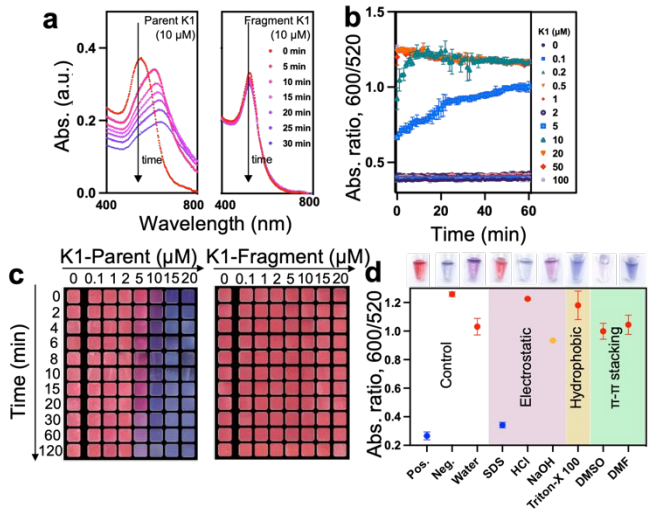

Figure 2. Characterization of peptide-AuNPs interaction. (a) The time progression of optical absorption of AuNPs when incubated with K1 parent (left) and fragment (right) peptides. Curves from red to purple were recorded every 5 min for 30 min. **(b)** Time progress of ratiometric absorbance of AuNPs when incubated with a serial concentration of K1 parent. Error bars represent the standard deviation (n=3). **(c)** Concentration and time-dependent colour evolution of DPPS-AuNPs in the presence of K1 parent peptide (left) and fragment (right). **(d)** White-light image (top) and quantified reversal color change (bottom) of the AuNPs pellet in different surfactant solutions (10 mM, 100 μL) or solvents (100 μL). These different solvents test different reasons for AuNP aggregation. Redispersion in SDS indicates that the dominant force is electrostatic forces.

Our previous work has explored the aggregation behaviour using Arg (R).[11] Both Lys and Arg are positively charged amino acids, with Lys already present in the cleavage sequence.[14] As a result, we formulated the K1 peptide by utilizing Lys as the positively charged amino acid, and then introduced a second K on the other end. This adjustment resulted in a charge valence of +2. The K2 peptide contained two positive charge domains at both N- and C- terminals but has a scrambled sequence, therefore there is no interaction with the protease (**Fig. S1a**). The K2 peptide validates that the colour change is specifically induced by SV3CP. The control peptides K3 and K4 possess the cleavable cleavage sequence: K3 has the two positive domains on the C-terminus, and K4 has only one positive domain at the C-terminus. These designs ensured the proteolysis while maintaining the same charge valence before and after proteolysis, which verifies that the colour change is from the charge valence difference. **Fig. S4b** shows the operational window of these peptides, and the result supports our hypothesis, *i.e.*, the aggregation/dispersion trend by control peptides is the same regardless of the presence of SV3CP.

The reverse dispersion experiment demonstrated the aggregation was driven by electrostatic interactions. In **Fig. 2d**, the aggregated pellet can be easily dissociated by sodium dodecyl sulphate (SDS). The anionic SDS can disrupt the electrostatic binding between peptides and AuNPs, thus restoring the electrostatic double-layer repulsions between the particles.[15] In addition, sodium hydroxide (NaOH) can slightly reverse the aggregation at around pH 11.0—this is likely due to the deprotonation of ammonium groups in Lys, which reduces the overall positive charge of the peptides and weakens the electrostatic interaction with the negatively charged AuNPs.[16] Neither of the hydrophobic and π-π stacking solvents can redisperse the pellets suggesting that the interaction between peptides and AuNPs is primarily from electrostatic reactions.

To study the limit of detection (LoD) for SV3CP, an enzyme assay was performed by incubating 10 μM of K1 with SV3CP for 8 hours in Tris buffer (0.02 M, pH 8.0, with 150 mM NaCl and 5 mM DTT). The DPPS-AuNPs were then added to report the colour. The kinetics are shown in **Fig. S4c** and clearly show that the absorbance ratio decreases with a higher concentration of enzymes. The LoD is 320 nM in Tris buffer (**Fig. 3a**). The LoD improved to 250 nM with a longer incubation time of 48 hours (**Fig. S2a**). To further characterize the proteolysis behaviour of the custom substrate, a synthetic fluorogenic substrate (Cy5.5-K1-Cy5.5) was used to determine the specificity constant (k_{cat}/K_M). The substrate has two Cy5.5 groups on each end flanking the K1 peptide with the self-quenching behaviour.[17] For our substrate, a specificity constant of 64.26 $M^{-1}s^{-1}$ was observed, which is in the range of reported value from the literature (**Fig. 3b**).[18] This indicates that the relatively high LoD could be due to low enzyme-substrate affinity.

We also performed a heat denaturation experiment to investigate the specificity of the biosensor to SV3CP. SV3CP was heated at 60˚C for 3 hours followed by incubation with the substrate for 8 hours.[19] The mixture did not induce coagulation suggesting that the protease itself cannot induce a colour change on the aggregated AuNPs; proteolysis is required for a colour change (**Fig. S5a**). We further cross-tested the incubation of substrate with a series of mammalian proteins against our sensing system including trypsin (*i.e.*, cleaves at C-terminus of Lys or Arg), thrombin (*i.e.*, cleaves the Arg-Gly bond in fibrinogen), hemoglobin, bovine serum albumin (BSA), and α-amylase (*i.e.*, digests α-1,4-glucosidic bond in starch) (**Fig. 3c**).[25] Trypsin showed a partial positive result (50%) because it can be active on the C-terminal of Lys. BSA and hemoglobin yielded a strong positive result. However, these two proteins are not expected to undergo proteolysis, and thus we incubated them with K1 parent peptide for 8 hours and analysed the sample using HPLC (**Fig. S5b**). The HPLC results demonstrated no proteolysis: All samples exhibited the same pattern. We thus concluded that the inhibition of aggregation in the presence of BSA and hemoglobin is attributed to the protein corona effect where proteins attach to the surface of AuNPs and stabilize them by electro-steric effect.[20]

We evaluated the matrix effects in a series of biological media by first spiking SV3CP into Tris buffer, BSA solution (1%), saliva, exhaled breath condensate (EBC), Dulbecco's modified Eagle medium (DMEM) cell culture media, urine, human plasma, and faecal matter (**Fig. 3d**). The negative controls where SV3CP was absent shows that DMEM, serum, and human plasma give false positive results from protein corona formation.[20] The biosensor exhibited excellent performance in Tris buffer, EBC, urine, and faecal matter. This is particularly significant since the detection of HNV primarily occurs in faecal matter.[21] Thus, the successful

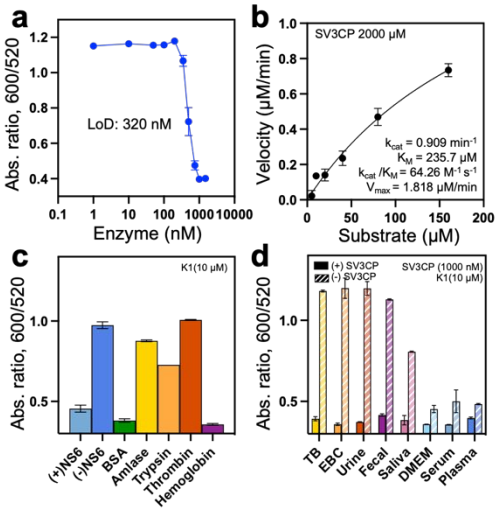

Figure 3. Performance in biological environment. (a) Ratiometric absorbance as a function of SV3CP concentration. The substrate was incubated with the protease in Tris buffer for 8 hours before the addition of DPPS-AuNPs. Error bars = standard deviation (n = 3). **(b)** k_{cat}/K_M determination of the hydrolysis of the fluorogenic substrate (Cy5.5-K1-Cy5.5) by SV3CP in 0.02 M Tris buffer (NaCl 150 mM, DTT 5 mM, pH 8.0). SV3CP (2000 nM) was incubated with varying fluorogenic substrate concentrations (e.g., 5-160 μM). Data was fitted to the Michaelis-Menten equation (**Equation S4**). **(c)** Sensor activation by mammalian proteins (1000 nM) in Tris buffer, including trypsin, thrombin, hemoglobin, BSA, and amylase. Sample with and without SV3CP served as positive and negative controls, respectively. **(d)** Sensor performance in other biological media. Negative controls without SV3CP are shown in a stripe pattern.

operation of our system in faecal matter represents a notable advancement. We also evaluated the LoD in EBC (472 nM), urine (221 nM), and faecal matter (267 nM) (**Fig. S6**).

Overall, we developed a straightforward and fast way to detect HNV that requires no complex procedure and equipment. The label-free biosensor shows several advantages over traditional detection methods. Unlike ELISA, which demonstrates low selectivity, or RT-PCR, which processes results through complex steps within up to 24 hours, our biosensor offers swifter results. Additionally, the biosensor's application extends beyond that of EM, which cannot be employed for analysing samples from food and environmental contaminants.[22] For future development, we could employ other nanoparticles, such as gold-silver nanoparticle alloys, to enhance the colour differentiation.

Conflicts of interest

There are no conflicts to declare.

Acknowledgements

TEM images were collected from Cellular and Molecular Medicine Electron Microscopy Core (UCSD-CMM-EM Core, RRID: SCR_022039) Cellular and Molecular Medicine Electron Microscopy Core (UCSD-CMM-EM Core, RRID: SCR_022039). The authors acknowledge the use of facilities and instrumentation supported by the National Science Foundation through the University of California San Diego Materials Research Science and Engineering Center DMR-2011924.

Notes and references

1 M. Alsved, C. J. Fraenkel, M. Bohgard, A. Widell, A. Soderlund-Strand, P. Lanbeck, T. Holmdahl, C. Isaxon, A. Gudmundsson, P. Medstrand, B. Bottiger and J. Londahl, Clin. Infect. Dis., 2020, 70, 2023-2028.
2 K. Debbink, L. C. Lindesmith and R. S. Baric, Clin. Infect. Dis., 2014, 58, 1746-1752.
3 J. A. Ayukekbong, H. N. Mesumbe, O. G. Oyero, M. Lindh and T. Bergstrom, J. Gen. Virol., 2015, 96, 1983-1999.
4 K. Pyrc, K. Stożek, K. Wojcik, K. Gawron, S. Zeglen, W. Karolak, J. Wojarski, M. Ochman, M. Hubalewska-Mazgaj, G. Bochenek, M. Sanak, M. Zembala, A. Szczeklik and J. Potempa, PLoS One, 2012, 7, e32582.
5 K. Akshaya, C. Arthi, A. J. Pavithra, P. Poovizhi, S. S. Antinate, G. S. Hikku, K. Jeyasubramanian and R. Murugesan, Photodiagnosis Photodyn. Ther., 2020, 30, 10.
6 H. Jing, Q. Zhang, N. Large, C. Yu, D. A. Blom, P. Nordlander and H. Wang, Nano Lett., 2014, 14, 3674-3682.
7 G. A. Smolyakov, P. G. Eliseev and M. Osinski, IEEE Journal of Quantum Electronics, 2005, 41, 517-524.
8 W. W. Chen, Y. M. Guo, W. S. Zheng, Y. L. Xianyu, Z. Wang and X. Y. Jiang, Chin. J. Anal. Chem., 2014, 42, 307-314.
9 L. F. Ludwig-Begall, A. Mauroy and E. Thiry, Viruses-Basel, 2021, 13, 36.
10 Z. Jin, Y. Li, K. Li, J. Zhou, J. Yeung, C. Ling, W. Yim, T. He, Y. Cheng, M. Xu, M. N. Creyer, Y.-C. Chang, P. Fajtová, M. Retout, B. Qi, S. Li, A. J. O'Donoghue and J. V. Jokerst, Angewandte Chemie International Edition, 2023, 62, e202214394.
11 Y.-C. Chang, Z. Jin, K. Li, J. Zhou, W. Yim, J. Yeung, Y. Cheng, M. Retout, M. N. Creyer, P. Fajtová, T. He, X. Chen, A. J. O'Donoghue and J. V. Jokerst, Chemical Science, 2023, 14, 2659-2668.
12 G. Schmid and A. Lehnert, Angewandte Chemie International Edition in English, 1989, 28, 780-781.
13 A. Heuer-Jungemann, N. Feliu, I. Bakaimi, M. Hamaly, A. Alkilany, I. Chakraborty, A. Masood, M. F. Casula, A. Kostopoulou, E. Oh, K. Susumu, M. H. Stewart, I. L. Medintz, E. Stratakis, W. J. Parak and A. G. Kanaras, Chem. Rev., 2019, 119, 4819-4880.
14 R. J. Hussey, L. Coates, R. S. Gill, P. T. Erskine, S.-F. Coker, E. Mitchell, J. B. Cooper, S. Wood, R. Broadbridge, I. N. Clarke, P. R. Lambden and P. M. Shoolingin-Jordan, Biochemistry, 2011, 50, 240-249.
15 J.-M. Jung, G. Savin, M. Pouzot, C. Schmitt and R. Mezzenga, Biomacromolecules, 2008, 9, 2477-2486.
16 Z. Jin, Y. Mantri, M. Retout, Y. Cheng, J. Zhou, A. Jorns, P. Fajtova, W. Yim, C. Moore, M. Xu, M. N. Creyer, R. M. Borum, J. Zhou, Z. Wu, T. He, W. F. Penny, A. J. O'Donoghue and J. V. Jokerst, Angewandte Chemie International Edition, 2022, 61, e202112995.
17 C. Moore, R. M. Borum, Y. Mantri, M. Xu, P. Fajtová, A. J. O'Donoghue and J. V. Jokerst, ACS Sensors, 2021, 6, 2356-2365.
18 P. Viswanathan, J. May, S. Uhm, C. Yon and B. Korba, Virology, 2013, 438, 20-27.
19 A. Hellysaz, M. Neijd, T. Vesikari, L. Svensson and M. Hagbom, mBio, 2023, 14, e03567-03522.
20 D. Baimanov, R. Cai and C. Y. Chen, Bioconjugate Chem., 2019, 30, 1923-1937.
21 G. Tung-Thompson, D. A. Libera, K. L. Koch, F. L. de Los Reyes, 3rd and L. A. Jaykus, PLoS One, 2015, 10, e0134277.
22 A. Knight, D. Li, M. Uyttendaele and L. A. Jaykus, Crit. Rev. Microbiol., 2013, 39, 295-309.